Combination band spectroscopy of H_3^+

Benjamin J. McCall[a] and Takeshi Oka
Department of Chemistry, Department of Astronomy & Astrophysics, and the Enrico Fermi Institute, University of Chicago, Chicago, Illinois 60637

(Received 9 May 2000; accepted 25 May 2000)

Thirty rovibrational transitions of H_3^+ have been observed near 1.25 μm using a tunable diode laser and a positive column discharge. In addition to the H_3^+ transitions, over 200 transitions between Rydberg states of H_2 were observed—these could be discriminated against by using a discharge dominated by He, which apparently collisionally quenches the Rydberg states of H_2 without affecting H_3^+. Twenty-eight of the H_3^+ transitions have been assigned to the $\nu_1+2\nu_2^2\leftarrow 0$ band, and provide experimentally determined energy levels for most of the levels up to $J=4$ in the $\nu_1+2\nu_2^2$ state. The remaining two H_3^+ transitions have been assigned to the $2\nu_1+\nu_2\leftarrow 0$ band. These bands represent a crucial test of *ab initio* calculations, as they reach higher vibrational levels of H_3^+ than any yet observed. We have compared our experimental results with recent variational calculations by several groups. © *2000 American Institute of Physics.* [S0021-9606(00)02132-2]

I. INTRODUCTION

H_3^+, the simplest stable polyatomic molecule, plays important roles in laboratory, theoretical, and astronomical spectroscopy. In the laboratory, H_3^+ is the primary positive charge carrier in hydrogen plasmas. The intense spectrum of H_3^+ has been used as a diagnostic of these plasmas, in order to measure the radial distribution of charge,[1] the rate of electron recombination,[2] and the rate of destruction of ions by ambipolar diffusion.[3] For theoreticians, H_3^+ serves as a benchmark for rovibrational calculations of polyatomic molecules[4–6]—indeed, *ab initio* theory is now approaching spectroscopic accuracy for this ion. Finally, H_3^+ plays a major role in astronomical plasmas, where its rovibrational spectrum serves as an important remote probe for studying the ionospheres of the outer planets[7,8] as well as dense[9–11] and diffuse[11–13] interstellar clouds.

These applications depend on accurate laboratory measurements of H_3^+ transition frequencies. Since the $\nu_2\leftarrow 0$ rotation–vibration band of H_3^+ was first detected in the laboratory,[14] work has continued to spectroscopically probe higher energy levels using hot bands, overtone bands, and forbidden bands. Spectroscopy of high energy levels of H_3^+ provides new data for comparison with theoretical predictions and also extends the list of transitions available for astronomical spectroscopy of hot plasmas (such as Jupiter's ionosphere). For more details on previous laboratory work, readers are referred to a recent review.[15]

In this paper we report our recent laboratory observation of the $\nu_1+2\nu_2^2\leftarrow 0$ (the superscript refers to $|l|$, as defined in the following) and $2\nu_1+\nu_2\leftarrow 0$ combination bands of H_3^+ near 1.25 μm using a tunable diode laser. These bands reach higher vibrational levels than any previous work, and therefore provide a new test of rovibrational calculations. This work sets the stage for the detection of the $5\nu_2\leftarrow 0$ overtone band, which probes the theoretically challenging area above the barrier to linearity.

II. THEORY AND NOTATION

The quantum numbers F (total angular momentum) and $\pm$ (parity) are rigorously good quantum numbers due to the isotropy and inversion symmetry of free space. Neglecting the very small nuclear spin–rotation interaction, we can write $F=I+J$ and consider I (total nuclear spin angular momentum) and J (angular momentum of nuclear and electronic motion) to be good quantum numbers. The electric dipole selection rules for these quantum numbers are $\Delta J=0$ or ± 1, $\Delta I=0$, and $+\leftrightarrow -$.

There are other quantum numbers that are approximately good at low energies. These include v_1 and v_2 (the number of quanta in the symmetric ν_1 stretching and the degenerate ν_2 mode) as well as $|l|$, the vibrational angular momentum of the ν_2 mode (the signed quantity l, which is not a good quantum number, runs from $v_2, v_2-2, \ldots, -v_2$). These three approximate quantum numbers $(v_1, v_2, |l|)$ collectively specify the vibrational state of H_3^+. We can also consider the quantity k, the (signed) component of J along the molecular symmetry axis.

The symmetry of H_3^+ is best considered using the S_3^* permutation-inversion group, which is isomorphic to the D_{3h} point group. The symmetry properties of the rovibrational wave functions with respect to the $(123)=C_3$ and $E^*=\sigma_h$ operations can be shown[16] to be

$$(123)|J,k,l\rangle = \exp\left[\frac{2\pi i}{3}(k-l)\right]|J,k,l\rangle \tag{1}$$

and

$$E^*|J,k,l\rangle = (-1)^k|J,k,l\rangle. \tag{2}$$

Based on Eq. (1), it is convenient to introduce the quantum number $g\equiv k-l$, which can be thought of physically as the component of J along the symmetry axis which is due to

[a]Electronic mail: bjmccall@uchicago.edu

rotation. The quantum number g is connected to the spin modification of H_3^+ ($g=3n$ is *ortho* [$I=3/2$] and $g=3n\pm1$ is *para* [$I=1/2$]) by the Pauli principle, which requires that the total (spin and rovibrational) wave function be antisymmetric with respect to the interchange of two protons (12) and symmetric with respect to cyclic permutation of all three protons (123). This requirement is equivalent to the requirement that the total wave function belong to the A_2 representation. A further consequence of the Pauli principle is that certain rovibrational levels (e.g., $J=$even, $G=0$ in the ground vibrational state) do not exist. Equation (2) shows that the parity is $+$ when k is even, and $-$ when k is odd.

Because the space-fixed electric dipole moment is invariant to (123) but changes sign with E^*,[17] it follows that the electric dipole selection rules for H_3^+ are

$$\Delta g \equiv \Delta(k-l)=3n \quad (n \text{ integer}) \text{ and } \Delta k=\text{odd}, \tag{3}$$

which are closely related to the original selection rules $\Delta I=0$, and $+\leftrightarrow-$.

For vibrational bands with $\Delta l=\pm1$ (e.g., $\nu_2\leftarrow0$), the selection rules (3) imply that $\Delta g=0$ and $\Delta k=\pm1$. For bands with $\Delta l=\pm2$ (e.g., $\nu_1+2\nu_2^2\leftarrow0$), the selection rules imply that $\Delta g=\mp3$ and $\Delta k=\mp1$. Bands with $\Delta l=0$ (e.g., $\nu_1+2\nu_2^0\leftarrow0$) are ''forbidden'' because they require $\Delta k=\pm3$ (and therefore $\Delta g=\pm3$) to satisfy Eq. (3) — however, some transitions in such ''forbidden'' bands can still be weakly observed due to intensity borrowing from ''allowed'' bands.

Since the energy is independent of the sign of g, the unsigned $G\equiv|g|$ is more often used. For vibrational bands with $l\neq0$, certain (J,G) levels are doubled, because there are two sets of k and l which give the same G. This occurs for $J>|l|$ and for $J-|l|\geqslant G\geqslant1$. In such cases it is convenient to label the upper and lower levels of each doublet as u and l (for ''upper'' and ''lower''). The labels u and l, respectively, replace the $+$ and $-$ labels previously used in the literature and correspond to $U=|l|$ and $-|l|$ (the U label was introduced by Watson[16] for $|l|=1$ and extended to $|l|>1$ by Miller and Tennyson[18]).

With this labeling, a new shorthand notation has recently been introduced[15] to describe rovibrational transitions of H_3^+. This notation consists of the vibrational band including $|l|$ as a superscript when $|l|\neq1$ (e.g., $\nu_1+2\nu_2^2\leftarrow0$) and an extension of the usual nomenclature $\{P|Q|R\}(J,G)$, where P, Q, and R as usual refer to $\Delta J=-1$, 0, and $+1$, respectively, and J and G refer to the lower state of the transition. If the upper level of the transition belongs to a doublet, then the appropriate u or l is appended as a superscript after the (J,G). Similarly, if the lower level belongs to a doublet, a u or l subscript is appended. For $\Delta g=\pm3$ bands, a superscript n or t is prepended to indicate $\Delta G=-3$ or $+3$, respectively. Note that for $G''=1$ and 2, the n transitions formally appear as $\Delta G=+1$ and -1, respectively. For $G''=0$ there are only t transitions.

Although they were not encountered in this work, transitions with $\Delta g=\pm3m$ ($m>1$) which can be observed due to intensity borrowing are denoted with a signed value of $|\Delta g|$ as a superscript in the place of n or t. In analogy with n and t, the sign is taken to be that of ΔG, except that the sign is always taken to be $-$ when G ''wraps around zero'' (e.g., $g=+4\leftarrow-2$).

III. EXPERIMENT

The experiment employed a custom-built external-cavity tunable diode laser from New Focus. When manufactured, the laser had a nominal tuning range of 7633–8183 cm^{-1}, but due to degradation of the antireflection coating on the front facet of the diode, it only had a useful tuning range of $\sim$7780–8168 cm^{-1} at the time of the observations. The effect of this degradation is most pronounced on the low frequency side of the tuning range, such that it is only possible to continuously tune the laser from about 7850 to 8168 cm^{-1}. At the center of its tuning range, the laser produces approximately 8 mW of radiation.

The H_3^+ was produced inside a liquid-nitrogen cooled discharge cell with an inner diameter of 18 mm and a length of approximately 1 m.[15] The reagent gas ($\sim$500 mTorr of H_2 and optionally $\sim$10 Torr of He) flowed into the cell through multiple inlets, and was pumped out through multiple outlets by a mechanical pump. The plasma was produced by a several kilovolt, 18 kHz ac potential applied across two electrodes, one on each side of the cell. This potential was produced by a step-up transformer driven by a Techron 7780 power amplifier (4 kW peak output), which was fed by a sine-wave generator. The discharge current was approximately 310 mA rms, which corresponds to a current density of $\sim$120 mA cm^{-2}. The use of an alternating current discharge allowed the velocity modulation technique[19] to be used to increase the sensitivity.

The output of the diode laser was split into two beams, which were sent through the discharge cell in opposite directions. Each beam was passed through the cell four times (with the same directionality each time) in order to increase the absorption path length without sacrificing the velocity modulation. The two beams were then directed into the two detectors of an autobalancing photoreceiver (New Focus Nirvana), which electronically balanced the signals from the two detectors in order to effect optimum cancellation of common-mode noise. The output of the photoreceiver was sent to a phase sensitive detector, which used the discharge sine-wave generator as the reference. The phase sensitive detector output was then digitized by a personal computer.

The diode laser was tuned by changing the angle of the cavity end mirror with respect to the grating. Coarse tuning was accomplished by a motor-turned screw, while fine tuning was effected by a piezoelectric transducer (PZT). The voltage on the PZT was controlled via a digital–analog converter in the PC, which enabled computer-controlled scanning of a 2 cm^{-1} range. The computer control of both tuning and data acquisition enabled multiple scans of each 2 cm^{-1} frequency range to be averaged together in order to reduce low frequency noise and produce a flatter baseline.

Each 2 cm^{-1} range was divided into 300 frequency steps (200 MHz each). While the bandwidth of the laser was far lower ($<$ 5 MHz), this interval was chosen as a tradeoff between spectral resolution and integration time. During each scan of the 2 cm^{-1} range, the computer instructed the

laser to move from one frequency step to the next. At each step, the computer averaged 100 samples of each experimental input, moved the laser to the next frequency step, and waited 30 ms before taking any more data. This delay time was chosen to be equal to the phase sensitive detector time constant. At the end of the 2 cm^{-1} range, the laser was instructed to return to the first frequency point and the computer waited for 1 s for the laser to stabilize.

Each scan of the 2 cm^{-1} range took approximately 10 s. The laser was extremely stable and reproducible in frequency, such that hundreds of scans could be averaged together when necessary to increase the signal-to-noise ratio. This corresponded to repeated scanning of the same frequency range for over 1 h.

Frequency calibration was achieved by simultaneously measuring the H_3^+ spectrum, an absorption spectrum of NH_3, and the transmission of a 2 GHz etalon. The etalon ticks were used for relative frequency calibration, and the NH_3 wave numbers of Guelachvilli[20] were used for absolute calibration. Observation of the Paschen β line of atomic hydrogen showed that there was a slight (0.017 cm^{-1}) shift between the modulated absorption lines and the direct absorption lines of NH_3, most likely caused by the time constant of the phase sensitive detector. This shift was found to be independent of the intensity of the absorption line, so this shift was adopted as a constant correction to our observed wave numbers.

IV. RESULTS

The entire frequency range between 7850 and 8168 cm^{-1} was scanned by overlapping individual 2 cm^{-1} scans. This scanning was performed with both a pure hydrogen discharge ($P_{H_2} \sim 500$ mTorr) and with a helium-dominated discharge ($P_{He} \sim 10$ Torr and $P_{H_2} \sim 500$ mTorr). In addition, individual 2 cm^{-1} scans were made at the frequencies in the range 7785–7850 cm^{-1} where strong lines were expected from the variational calculations of Watson.[21]

The experiment yielded 30 rovibrational transitions of H_3^+ as well as over 200 transitions between Rydberg states of H_2 (denoted H_2^*). A table of the Rydberg transitions and their intensities can be obtained from the EPAPS archive.[22] The Rydberg transitions generally appeared with the phase of negative ions, because H_2^* is formed by impact with electrons.[23] About 10% of the Rydberg lines, however, appeared with the same phase as positive ions. This is interpreted[24] as being due to stimulated emission of transitions between triplet states of H_2^* — the dissociative character of the lower state leads to the necessary population inversion.

Because some Rydberg transitions appear with the same phase as the H_3^+ transitions, the phase alone is not enough to discriminate between H_3^+ and H_2^*. However, the addition of He (10 Torr) as a buffer gas decreases the intensity of the H_2^* lines by about a factor of 30 while not significantly affecting the intensity of the H_3^+ lines, as demonstrated in Fig. 1. This decrease can be largely attributed to the factor of 20 increase in gas pressure, which provides more collisions to quench the H_2^*. Because of the very low proton affinity of He (1.85 eV) compared to that of H_2 (4.39 eV), the amount of H_3^+ is not reduced by the addition of He to the discharge. By scanning each spectral region in both a pure hydrogen discharge as well as a helium-dominated discharge, we are able to unambiguously identify the H_3^+ lines.

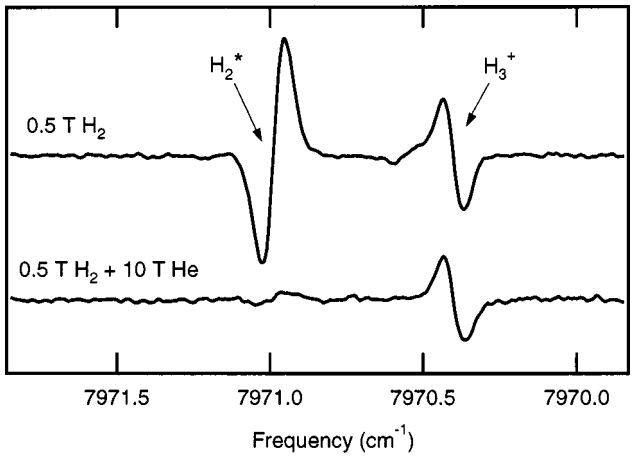

FIG. 1. Effect of He on H_2^* and H_3^+ [$^tR(1,0)$] absorption lines.

The observed H_3^+ transitions and their assignments are listed in Table I. Twenty-six of the assignments could be made by a simple comparison with Watson's calculations.

TABLE I. Observed frequencies and assignments.

Frequency[a]	Assignment	Band	J'	$\langle G' \rangle$[b]	J''	K''
7785.233 (10)	$^tQ(3,0)$	$\nu_1+2\nu_2^2 \leftarrow 0$	3	3.0	3	0
7785.701 (10)	$^tQ(1,0)$	$\nu_1+2\nu_2^2 \leftarrow 0$	1	3.0	1	0
7789.878 (10)	$^tR(3,3)$	$\nu_1+2\nu_2^2 \leftarrow 0$	4	5.9	3	3
7805.893 (10)	$^nP(1,1)$	$\nu_1+2\nu_2^2 \leftarrow 0$	0	2.0	1	1
7820.239 (10)	$^nP(2,2)$	$\nu_1+2\nu_2^2 \leftarrow 0$	1	1.0	2	2
7822.375 (10)	$^tR(2,2)$	$\nu_1+2\nu_2^2 \leftarrow 0$	3	5.0	2	2
7826.739 (10)	$^nP(3,3)$	$\nu_1+2\nu_2^2 \leftarrow 0$	2	0.0	3	3
7833.249 (20)	$^nP(4,4)^l$	$\nu_1+2\nu_2^2 \leftarrow 0$	3	1.1	4	4
7850.959 (10)	$^tR(1,1)$	$\nu_1+2\nu_2^2 \leftarrow 0$	2	4.0	1	1
7880.921 (10)	$^tR(4,3)$	$\nu_1+2\nu_2^2 \leftarrow 0$	5	5.9	4	3
7894.711 (10)	$^nQ(1,1)$	$\nu_1+2\nu_2^2 \leftarrow 0$	1	2.0	1	1
7898.371 (10)	$^nQ(2,1)$	$\nu_1+2\nu_2^2 \leftarrow 0$	2	2.0	2	1
7905.717 (10)	$^nQ(3,1)$	$\nu_1+2\nu_2^2 \leftarrow 0$	3	2.0	3	1
7912.047 (10)	$^tR(3,2)$	$\nu_1+2\nu_2^2 \leftarrow 0$	4	4.9	3	2
7939.619 (10)	$^tR(2,1)$	$\nu_1+2\nu_2^2 \leftarrow 0$	3	4.0	2	1
7970.413 (10)	$^tR(1,0)$	$\nu_1+2\nu_2^2 \leftarrow 0$	2	3.0	1	0
7998.890 (10)	$^nQ(2,2)$	$\nu_1+2\nu_2^2 \leftarrow 0$	2	1.0	2	2
8005.582 (30)	$^tR(4,2)$	$\nu_1+2\nu_2^2 \leftarrow 0$	5	4.8	4	2
8007.410 (10)	$^nQ(3,2)^u$	$\nu_1+2\nu_2^2 \leftarrow 0$	3	1.0	3	2
8022.012 (20)	$^nQ(4,2)^u$	$\nu_1+2\nu_2^2 \leftarrow 0$	4	1.0	4	2
8027.840 (20)	$^tR(3,1)$	$\nu_1+2\nu_2^2 \leftarrow 0$	4	3.5	3	1
8037.673 (10)	$^nR(3,1)^l$	$\nu_1+2\nu_2^2 \leftarrow 0$	4	2.4	3	1
8053.382 (10)	$P(6,6)$	$2\nu_1+\nu_2 \leftarrow 0$	5	5.5	6	6
8071.617 (10)	$^nR(1,1)$	$\nu_1+2\nu_2^2 \leftarrow 0$	2	2.0	1	1
8089.406 (10)	$^nQ(4,3)$	$\nu_1+2\nu_2^2 \leftarrow 0$	4	0.1	4	3
8110.069 (10)	$^nQ(3,3)$	$\nu_1+2\nu_2^2 \leftarrow 0$	3	0.0	3	3
8123.128 (10)	$P(5,5)$	$2\nu_1+\nu_2 \leftarrow 0$	4	4.8	5	5
8128.280 (10)	$^tR(4,1)$	$\nu_1+2\nu_2^2 \leftarrow 0$	5	3.4	4	1
8162.653 (10)	$^tR(3,0)$	$\nu_1+2\nu_2^2 \leftarrow 0$	4	2.9	3	0
8163.129 (10)	$^nR(2,1)$	$\nu_1+2\nu_2^2 \leftarrow 0$	3	2.0	2	1

[a]The uncertainty in the last decimal places is listed in parentheses.
[b]The expectation value of the approximate quantum number G in the upper state, from the calculations of Watson (Ref. 21).

However, there were two pairs of lines (7785.233 and 7785.701; 8162.653 and 8163.129) which were too close in frequency to assign solely by comparison with the calculated frequencies. The first pair of lines was assigned based on the temperature dependence of the observed intensities: the lower frequency line became more intense in the helium-dominated (hotter) discharge and therefore arises from the $(J=3, K=0)$ level in the ground state, rather than $(J=1, K=0)$. The second pair was assigned based on combination differences: the higher frequency line of the pair shares the same upper state as the line at 7905.717 cm^{-1}.

Table I also shows the uncertainties in the experimental frequencies, which have been estimated by comparing the frequencies obtained in different scans and by considering the proximity of NH_3 reference lines. Also listed in Table I are the values of J and K in the ground state, along with the values of J and the expectation value of the approximate quantum number G in the upper state. These values are taken from the calculations of Watson.[21]

Based on these assignments, 28 of the 30 H_3^+ lines belong to the $\nu_1+2\nu_2^2\leftarrow 0$ band, while two are high-J P-branch lines of the $2\nu_1+\nu_2\leftarrow 0$ band, which has its band center[25] near 8487 cm^{-1}. The strongest line in the $\nu_1+2\nu_2^2\leftarrow 0$ band (7970.413 cm^{-1}) was detected with a signal-to-noise ratio of nearly 100. Considering that this band is approximately 270 times less intense than the fundamental band,[26] which is a few percent deep in absorption under similar conditions, we estimate that our sensitivity (minimum detectable absorption) is of order $\Delta I/I\sim 3\times 10^{-6}$. Our sensitivity was hampered by a persistent square-wave shaped noise in the intensity of the diode laser, which may have been due to optical feedback. This noise appeared most prominently when the multiple path optical arrangement was used. Because of the square-wave nature of the noise, it was not completely filtered out by the phase sensitive detection and thus contributed to noise in our baseline.

The experimentally determined energy levels, based on our observed transitions and the previously determined[27] ground state energy levels, are listed in Table II. In this table, we have listed the value of G for the member of the $|J,G\rangle$ basis set which makes the dominant contribution to the energy level. An energy level diagram of the $\nu_1+2\nu_2^2$ state is given in Fig. 2, where the observed levels are denoted by thick lines. The observed transitions provide nearly complete coverage up to $J=4$, along with three levels of $J=5$.

TABLE II. Experimentally determined energy levels.

v_1	v_2	l	J	G[a]	u/l[b]	E
1	2	2	0	2		7870.018
1	2	2	1	3		7872.664
1	2	2	2	4		7915.084
1	2	2	1	2		7958.836
1	2	2	1	1		7989.541
1	2	2	3	5		7991.677
1	2	2	2	3		8057.376
1	2	2	4	6		8105.230
1	2	2	2	2		8135.736
1	2	2	2	0		8142.091
1	2	2	2	1		8168.192
1	2	2	3	4		8176.978
1	2	2	3	3		8302.114
1	2	2	3	1	l	8335.291
1	2	2	4	5		8340.068
1	2	2	3	2		8400.488
1	2	2	3	0		8425.421
1	2	2	3	1	u	8435.431
1	2	2	4	4		8522.611
1	2	2	4	2	l	8532.444
1	2	2	5	6		8539.638
1	2	2	4	3		8679.534
1	2	2	4	0		8748.123
1	2	2	5	5		8774.053
1	2	2	4	1	u	8790.483
1	2	2	5	4		8961.857
2	1	1	4	5		8852.148
2	1	1	5	6		9049.257

[a]The value of G for the member of the $|J,G\rangle$ basis set which makes the dominant contribution to the energy level.
[b]Label for upper and lower states of doublets.

V. ANALYSIS

The primary motivation for this work was to provide experimental data on the $\nu_1+2\nu_2^2\leftarrow 0$ band for comparison with theoretical calculations. In this section, we briefly discuss several sets of variational calculations performed in recent years and compare them to our observed spectra. We also examine some previously observed lines that have been assigned to transitions involving the $\nu_1+2\nu_2^2$ state.

A. Comparison with variational calculations

We have compared our experimental H_3^+ frequencies with several sets of variational calculations. For each transition we compute the difference of the observed and calculated frequencies [observed−calculated (o−c)]. The average of the (o−c) values for all of the lines can be interpreted simply as an offset in the band origin, perhaps due to omission of various (adiabatic and/or nonadiabatic) corrections to the Born–Oppenheimer approximation and, to a lesser extent, relativistic corrections. The standard deviation σ(o−c) of the (o−c) values gives an indication of the accuracy of the calculation of the rovibrational energies (given some vibrational offset), and should be regarded as the primary figure of merit. The values of (o−c) for each line and for each calculation are tabulated in Table III, along with the average (o−c) and σ(o−c) for each calculation.

The earliest work we have considered in our comparison is that of Wolniewicz and Hinze (1994).[28] These authors calculated rotation-vibration term values up to $J=4$ using the Meyer-Botschwina–Burton (MBB)[29] *ab initio* potential and hyperspherical coordinates. The upper states of 19 of our observed transitions were listed in their table. Their average (o−c) was -0.25 cm^{-1}, which was less than the standard deviation σ(o−c)=0.30 cm^{-1}.

In 1996, Watson[21] provided us with theoretical predictions for the frequency range of this experiment. These calculations are an updated version of those discussed by Majewski *et al.*[30] and use a ''spectroscopically adjusted'' adaptation of the MBB[29] potential in which the potential constants have been adjusted to achieve a better fit between experiment and the variational calculations. These calculations were essential for conducting the experiment, as the

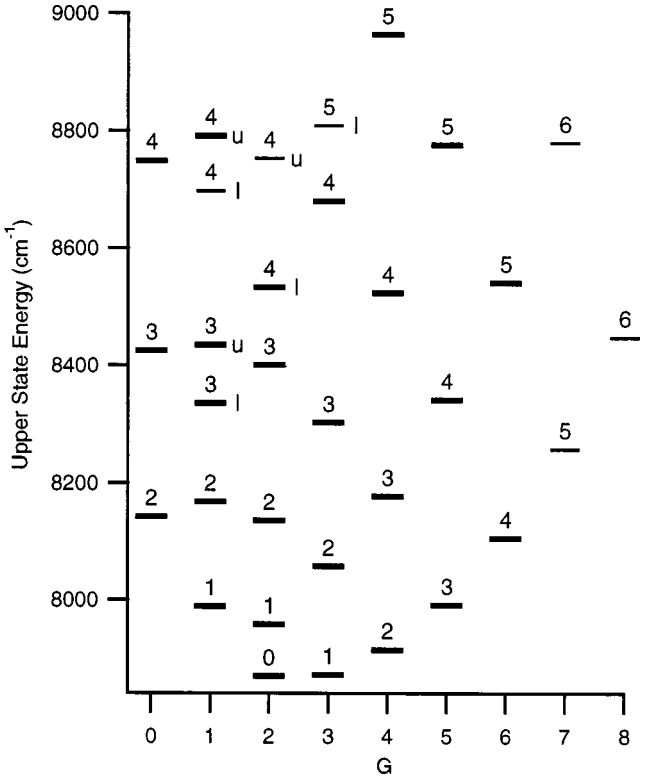

FIG. 2. Energy level diagram of the $\nu_1+2\nu_2^2$ state of H_3^+. Experimentally determined energy levels are denoted by thick lines. The values of J are indicated above the energy levels, and the u and l labels are to the right of the appropriate levels.

frequencies and relative intensities were completely reliable. No lines were observed in our region which were not predicted by Watson's calculations, and we observed all of the lines Watson predicted, given our sensitivity. We relied heavily on these calculations in determining where to focus our efforts outside of the continuous tuning range of the laser. A further advantage of Watson's calculations is that they provide the expectation values of the approximate quantum numbers v_1, v_2, l, and G, which make it easy to assign the energy levels and determine when the levels are strongly mixed. The average (o−c) was -0.23 cm^{-1}, which again was less than σ(o−c) = 0.47 cm^{-1}.

We also compared our data to the exhaustive line list of Neale, Miller, and Tennyson (1996) (NMT),[31] which was developed in part to facilitate opacity calculations of cool stars and the outer planets. These variational calculations are based on the spectroscopically adjusted potential of Dinelli, Polyansky, and Tennyson.[32] Their line list is somewhat difficult to use, as it only provides the value of J and the energy for the upper and lower levels of each transition. In some cases, even the spin modification (*ortho* or *para*) is not listed. For these reasons, their line list can only be interpreted by comparing the energies and J to those in other calculations which give more information about the levels. Their calculations included all 30 of our observed transitions, along with 37 400 others in this wave number range. Despite these reservations, the calculated frequencies of NMT are quite good: their average (o−c) was -0.33 cm^{-1}, and their σ(o−c) was only 0.09 cm^{-1}.

In 1997, Dinelli *et al.*[33] published a list of term values calculated in three different ways. They first used the DVR3D program suite on a spectroscopically adjusted potential[32] which is equivalent to the calculations of NMT. Second, they used the TRIATOM suite on the same potential. Third, they used the TRIATOM suite on the *ab initio* potential surface of Röhse *et al.*[34] augmented by *ab initio* non-Born–Oppenheimer adiabatic corrections.[35] Their list of term values contains some labeling errors, but is fairly comprehensive up to near 9000 cm^{-1}. Twenty-six of our observed lines could be calculated from their TRIATOM lists. The TRIATOM calculations on the spectroscopically adjusted potential gave an average (o−c) of -0.32 cm^{-1} and a σ(o−c) of 0.08 cm^{-1}. Their TRIATOM *ab initio* calculations gave a larger band origin offset [average (o−c)$=-0.74$ cm^{-1}] but a better standard deviation [σ(o−c)$=0.06$ cm^{-1}].

In 1999, Polyansky and Tennyson[5] published a new list of energy levels using the improved *ab initio* potential of Cencek *et al.*,[36] which includes electronic relativistic and adiabatic corrections. Polyansky and Tennyson also introduced nonadiabatic corrections in these calculations. Only 22 of our observed lines could be calculated from their list, and the fit was less satisfactory than the *ab initio* work of Dinelli *et al.*[33] The average (o−c) was 0.52 cm^{-1}, and the σ(o−c) was 0.18 cm^{-1}.

Very recently, Jaquet[37] has performed similar calculations based on the Cencek *et al.*[36] *ab initio* potential. Additionally, he calculated intensities using the dipole moment of Röhse *et al.*,[34] and these were found to be completely consistent with the experimental measurements. His calculations reproduced 29 of the 30 observed lines, with an average (o−c) of 0.53 cm^{-1} and a σ(o−c) of 0.09 cm^{-1}. In subsequent calculations, Jaquet included nonadiabatic corrections as discussed in Ref. 38. These corrections substantially reduced the band origin offset to an average (o−c) of 0.12 cm^{-1}, without changing the standard deviation.

By far the greatest deviation between the experimental and theoretical frequencies is for the $^nP(1,1)$ line observed at 7805.893 cm^{-1}. This transition is the only one going into $J=0$ in the $\nu_1+2\nu_2^2$ state. Jaquet[37] has suggested that this deviation may be due to the fact that the nonadiabatic correction should be smaller for the $J=0$ level. Calculations without nonadiabatic corrections will not reproduce this effect, and perhaps even the calculations with nonadiabatic corrections are not fully taking this into account. If the $J=0$ line is excluded from the comparison with the theoretical predictions, the standard deviations of NMT, Dinelli *et al.*, and Jaquet improve significantly. In fact, the *ab initio* calculation of Dinelli *et al.*[33] has a σ(o−c) of only 0.014 cm^{-1} when $J=0$ is excluded — this is comparable to the experimental accuracy.

B. Other assignments

With the energy levels of the $\nu_1+2\nu_2^2$ levels now experimentally determined, it is possible to evaluate some previously observed lines which have been assigned by other authors to transitions involving $\nu_1+2\nu_2^2$.

The transition $^tP(5,3)_l$ in the $\nu_1+2\nu_2^2\leftarrow 2\nu_2^2$ band has

TABLE III. Comparison with variational calculations.

Transition	Observed (cm^{-1})	(o−c) Adjusted Potentials W96[a]	N96[b]	D97a[c]	*Ab initio* Potentials WH94[d]	D97b[e]	P99[f]	J00a[g]	J00b[h]
$^tQ(3,0)$	7785.233	−0.032	−0.297	−0.295	−0.347	−0.714	0.571	0.507	0.138
$^tQ(1,0)$	7785.701	0.361	−0.309	−0.307	−0.326	−0.721	0.528	0.490	0.122
$^tR(3,3)$	7789.878	−0.147	−0.282	−0.233		−0.715	0.541	0.495	0.085
$^nP(1,1)$	7805.893	0.043	−0.647	−0.645	−0.465	−1.038		0.175	−0.221
$^nP(2,2)$	7820.239	0.259	−0.351	−0.356	0.043	−0.738	0.569	0.488	0.116
$^tR(2,2)$	7822.375	0.125	−0.265	−0.251		−0.708		0.513	0.105
$^nP(3,3)$	7826.739	0.060	−0.381	−0.377	0.269	−0.741	0.635	0.494	0.160
$^nP(4,4)^l$	7833.249	−0.195	−0.421	−0.421	0.293	−0.745	0.693	0.497	0.189
$^tR(1,1)$	7850.959	0.283	−0.291	−0.284		−0.719	0.514	0.510	0.103
$^tR(4,3)$	7880.921	−0.522	−0.259	−0.214		−0.711		0.535	0.092
$^nQ(1,1)$	7894.711	0.333	−0.339	−0.335	−0.186	−0.737	0.527	0.510	0.154
$^nQ(2,1)$	7898.371	0.183	−0.329	−0.329	−0.266	−0.735	0.525	0.511	0.079
$^nQ(3,1)$	7905.717	−0.174	−0.313	−0.310	−0.378	−0.725	0.542	0.531	0.172
$^tR(3,2)$	7912.047	−0.148	−0.243	−0.242		−0.714	−0.241	0.541	0.099
$^tR(2,1)$	7939.619	0.120	−0.271	−0.268		−0.713	0.532	0.547	0.135
$^tR(1,0)$	7970.413	0.288	−0.287	−0.285	−0.455	−0.717	0.506	0.549	0.112
$^nQ(2,2)$	7998.890	0.136	−0.350	−0.346	−0.050	−0.729	0.568	0.552	0.198
$^tR(4,2)$	8005.582	−0.858	−0.248					0.581	0.105
$^nQ(3,2)^u$	8007.410	−0.218	−0.350	−0.344	−0.260	−0.729		0.559	0.020
$^nQ(4,2)^u$	8022.012	−0.681	−0.318	−0.318	−0.426	−0.694	0.608	0.605	0.343
$^tR(3,1)$	8027.840	−0.497	−0.250	−0.244	−0.812	−0.698	0.550	0.602	0.015
$^nR(3,1)^l$	8037.673	−0.518	−0.337	−0.335		−0.754	0.538	0.551	0.153
$P(6,6)$	8053.382	−1.428	−0.528						
$^nR(1,1)$	8071.617	0.203	−0.313	−0.316	−0.247	−0.720	0.538	0.579	0.085
$^nQ(4,3)$	8089.406	−0.876	−0.344	−0.344	0.034	−0.724	0.665	0.596	0.168
$^nQ(3,3)$	8110.069	−0.133	−0.381	−0.384	−0.079	−0.725	0.600	0.596	0.144
$P(5,5)$	8123.128	−0.857	−0.492					0.372	0.259
$^tR(4,1)$	8128.280	−1.051	−0.270					0.604	0.007
$^tR(3,0)$	8162.653	−0.666	−0.257	−0.261	−0.780	−0.722	0.483	0.609	0.101
$^nR(2,1)$	8163.129	−0.166	−0.311	−0.310	−0.369	−0.721	0.542	0.612	0.158
Average (o−c)		−0.226	−0.334	−0.321	−0.253	−0.735	0.524	0.528	0.116
σ(o−c)		0.468	0.089	0.083	0.295	0.063	0.178	0.086	0.095
σ(o−c) [no $J=0$]		0.482	0.069	0.052	0.306	0.014	—	0.052	0.070

[a]Reference 21.
[b]Reference 31.
[c]Reference 33 (adjusted potential).
[d]Reference 28.
[e]Reference 33 (*ab initio*).
[f]Reference 5.
[g]Reference 37 (*ab initio*).
[h]Reference 37 (*ab initio* + nonadiabatic).

been assigned by Majewski *et al.*[30] to an observed line at 2134.241 cm^{-1}, but has also been assigned by Dinelli *et al.*[33] to an observed line at 2134.607 cm^{-1}. Based on the energy of the ($J=4$, $G=6$) level of $\nu_1+2\nu_2^2$ from this work and the energy of the lower level determined by Xu, Gabrys, and Oka,[27] we calculate that this transition should occur at 2134.000 cm^{-1}. This casts doubt on both assignments, but particularly on that of Dinelli *et al.*

Dinelli *et al.* have also assigned an observed line at 2403.350 cm^{-1} to the $Q(2,3)$ transition of the $\nu_1+2\nu_2^2 \leftarrow \nu_1+\nu_2$ band. Based on our experimental energy of the ($J=2$, $G=3$) level of $\nu_1+2\nu_2^2$ and the previously determined energy of the lower level,[39] we calculate that this transition should occur at 2403.367 cm^{-1}. Given the experimental uncertainties, this assignment cannot be excluded. In addition, Dinelli *et al.* assigned an observed line at 2648.105 cm^{-1} to the $R(2,3)$ transition of the same band. We calculate that this transition should occur at 2648.105 cm^{-1}, which confirms the assignment.

VI. CONCLUSIONS

Variational calculations of H_3^+ transitions using *ab initio* potential energy surfaces [as well as non-Born–Oppenhemier corrections] are beginning to approach experimental accuracy, especially when allowance is made for an offset in the band origin and the $J=0$ level. Improvements in the treatment of nonadiabatic effects will likely lead to even better agreement in the future.

The next frontier of H_3^+ spectroscopy lies at even higher energies ($\geqslant$10000 cm^{-1}), where H_3^+ has enough energy to sample linear geometries in the course of its vibrational mo-

tion. This energy regime is particularly difficult theoretically — none of the rovibrational variational calculations performed in this range to date include the correct boundary conditions for linear geometries. All of the vibrational states which have been spectroscopically probed to date (ν_2, ν_1, $2\nu_2^0$, $2\nu_2^2$, $\nu_1+\nu_2$, $3\nu_2^1$, $\nu_1+2\nu_2^2$, and $2\nu_1+\nu_2$) have been well below the barrier to linearity.

However, the detection of the $\nu_1+2\nu_2^2\leftarrow 0$ band with high signal to noise suggests that this barrier may soon be broken. The $5\nu_2^1\leftarrow 0$ band is expected to lie near 10 900 cm^{-1} ($\sim$920 nm) and should be only about a factor of 20 weaker than $\nu_1+2\nu_2^2\leftarrow 0$. With the much higher power and lower noise of the titanium:sapphire laser (compared to diode lasers), the detection of the $5\nu_2^1\leftarrow 0$ band may be within reach.

ACKNOWLEDGMENTS

We thank J. K. G. Watson and R. Jaquet for sending us the results of their calculations in advance of publication, as well as for many helpful discussions. We also thank G. Guelachvilli, who kindly provided the NH_3 frequency standard list that made this work possible. We would also like to acknowledge T. Huet and C. M. Lindsay for their assistance in the laboratory. This work was supported by NSF Grant No. PHYS-9722691 and NASA Grant No. NAG5-4070. B. J. M. is supported by the Fannie and John Hertz Foundation.

[1] F.-S. Pan and T. Oka, Phys. Rev. A **36**, 2297 (1987).
[2] T. Amano, Astrophys. J. **320**, L121 (1988).
[3] C. M. Lindsay, E. T. White, and T. Oka, Chem. Phys. Lett. (submitted).
[4] R. Jaquet, W. Cencek, W. Kutzelnigg, and J. Rychlewski, J. Chem. Phys. **108**, 2837 (1998).
[5] O. L. Polyansky and J. Tennyson, J. Chem. Phys. **110**, 5056 (1999).
[6] J. K. G. Watson, Chem. Phys. **190**, 291 (1995).
[7] J. Connerney, Philos. Trans. R. Soc. London, Ser. A (in press).
[8] S. Miller *et al.*, Philos. Trans. R. Soc. London, Ser. A (in press).
[9] T. R. Geballe and T. Oka, Nature (London) **384**, 334 (1996).
[10] B. J. McCall, T. R. Geballe, K. H. Hinkle, and T. Oka, Astrophys. J. **522**, 338 (1999).
[11] B. J. McCall, K. H. Hinkle, T. R. Geballe, and T. Oka, Faraday Discuss. **109**, 267 (1998).
[12] B. J. McCall, T. R. Geballe, K. H. Hinkle, and T. Oka, Science **279**, 1910 (1998).
[13] T. R. Geballe, B. J. McCall, K. H. Hinkle, and T. Oka, Astrophys. J. **510**, 251 (1999).
[14] T. Oka, Phys. Rev. Lett. **45**, 531 (1980).
[15] B. J. McCall, Philos. Trans. R. Soc. London, Ser. A (in press).
[16] J. K. G. Watson, J. Mol. Spectrosc. **103**, 350 (1984).
[17] J. T. Hougen, J. Chem. Phys. **37**, 1433 (1962).
[18] S. Miller and J. Tennyson, J. Mol. Spectrosc. **128**, 530 (1988).
[19] C. S. Gudeman, M. H. Begemann, J. Pfaff, and R. J. Saykally, Phys. Rev. Lett. **50**, 727 (1983).
[20] G. Guelachvilli (private communication).
[21] J. K. G. Watson (private communication).
[22] See EPAPS Document No. E-JCPSA6-113-021032 for a file containing the frequencies and intensities of the observed Rydberg transitions. This document may be retrieved via the EPAPS homepage (http://www.aip.org/pubservs/epaps.html) or from ftp.aip.org in the directory /epaps/. See the EPAPS homepage for more information. The table is also available on the author's web site (at http://h3plus.uchicago.edu/data/rydbergs.html).
[23] D. Uy, Ph.D. thesis, University of Chicago, 1998.
[24] D. Uy, C. M. Gabrys, T. Oka, B. J. Cotterell, R. J. Strickland, and Ch. Jungen (unpublished).
[25] B. M. Dinelli, S. Miller, and J. Tennyson, J. Mol. Spectrosc. **163**, 71 (1994).
[26] B. M. Dinelli, S. Miller, and J. Tennyson, J. Mol. Spectrosc. **153**, 718 (1992).
[27] L.-W. Xu, C. Gabrys, and T. Oka, J. Chem. Phys. **93**, 6210 (1990).
[28] L. Wolniewicz and J. Hinze, J. Chem. Phys. **101**, 9817 (1994).
[29] W. Meyer, P. Botschwina, and P. Burton, J. Chem. Phys. **84**, 891 (1986).
[30] W. A. Majewski, A. R. W. McKellar, D. Sadovskiĭ, and J. K. G. Watson, Can. J. Phys. **72**, 1016 (1994).
[31] L. Neale, S. Miller, and J. Tennyson, Astrophys. J. **464**, 516 (1996).
[32] B. M. Dinelli, O. L. Polyansky, and J. Tennyson, J. Chem. Phys. **103**, 10433 (1995).
[33] B. M. Dinelli, L. Neale, O. L. Polyansky, and J. Tennyson, J. Mol. Spectrosc. **181**, 142 (1997).
[34] R. Röhse, W. Kutzelnigg, R. Jaquet, and W. Klopper, J. Chem. Phys. **101**, 2231 (1994).
[35] B. M. Dinelli, C. B. Le Sueur, J. Tennyson, and R. D. Amos, Chem. Phys. Lett. **232**, 295 (1995).
[36] W. Cencek, J. Rychlewski, R. Jaquet, and W. Kutzelnigg, J. Chem. Phys. **108**, 2831 (1998).
[37] R. Jaquet (private communication).
[38] R. Jaquet, Chem. Phys. Lett. **302**, 27 (1999).
[39] L.-W. Xu, M. Rösslein, C. M. Gabrys, and T. Oka, J. Mol. Spectrosc. **153**, 726 (1992).